1-1-1996

Scanning-tunneling-microscopy study of faceting on high-step-density TaC surfaces

J.-K. Zuo
Missouri State University

J. Carpinelli

D. M. Zehner

J. F. Wendelken

Scanning-tunneling-microscopy study of faceting on high-step-density TaC surfaces

J.-K. Zuo
Department of Physics and Astronomy, Southwest Missouri State University, Springfield, Missouri 65804

J. M. Carpinelli
Department of Physics, University of Pennsylvania, Philadelphia, Pennsylvania 19104

D. M. Zehner and J. F. Wendelken
Solid State Division, Oak Ridge, National Laboratory, Oak Ridge, Tennessee 37831

(Received 27 November 1995)

We have studied the morphologies of the TaC(310), (210), and (110) surfaces using scanning tunneling microscopy. Heating the crystals to high temperatures activates a faceting of these surfaces into a hill-and-valley structure consisting of enlarged (100) terraces and (010) step walls. Step-separation distributions obtained from these surfaces can be well fit by sharp Gaussians and are much narrower than predicted for the noninteracting terrace-step-kink model, indicating a strong repulsive interaction exists between steps on the faceted surfaces. This faceting is suggested to be driven by a decrease in the total step repulsive energy through a reduction of the total number of step pairs. [S0163-1829(96)02723-3]

I. INTRODUCTION

Equilibrium crystal shapes have long been studied, dating back at least to Wulff's paper in 1901.[1] Early work was more based on thermodynamics which predicts equilibrium shapes with given surface free energies. For example, Herring showed[2] that if a surface does not coincide in orientation with some portion of the boundary of the equilibrium crystal shape, it would phase separate into a hill-and-valley structure which has a lower free energy than the original surface. The hill-and-valley structure can consist of two step-bunched facets (type I),[3,4] a high-symmetry terrace and a step-bunched facet (type II),[5–8] or two high-symmetry terraces (type III).[9,10] The high-symmetry terraces correspond to cusps in a Wulff plot. In addition to thermodynamics, the detailed calculation of surface free energy requires statistical mechanics, which views the problem microscopically.[11–17] One important factor to the surface free energy is steps. Interaction between steps contributes the third- and higher-order terms in the expansion of the free energy with respect to the step density.[12] Most reported facetings belong to either type-I or -II phenomena and have been observed on elemental metal and semiconductor surfaces. These facetings are usually induced by thermal treatment[6–8] and impurity absorption.[4,5] Thus far, however, the stability of ionic crystal surfaces has not been widely studied. In this paper, we report our scanning-tunneling-microscopy (STM) study of type-III faceting which occurs on the clean TaC(310), (210), and (110) surfaces. We will provide evidence that this faceting lowers the total step-step repulsive energy by reducing the total number of step pairs. This step-pair reduction is achieved by enlarging (100) terrace widths and (010) step-wall heights, while preserving the net surface orientation (see Fig. 1). Because the (100) and (010) crystal faces correspond to different cusps in the Wulff plot, this reconstruction can be viewed as an orientational phase separation from the bulk truncation. When the repulsive energy between a pair of single-height steps becomes larger than the formation energy of a single multiheight step on a high-step-density surface, orientational phase separation, or faceting, will occur. This picture has already been implied in discussions for the single- to double-height step phase transition on Si(100) with increasing step density.[15]

The nature of the step-step interaction can be determined from the step-separation distribution.[13] A repulsive step-step interaction can be deduced from two facts: (1) The step-separation distribution is single peaked and narrower than a ''universal'' distribution for the noninteracting terrace-step-kink (TSK) model.[14] This model neglects any energetic step-step interaction, but includes an effective entropic interaction between steps.[18] (2) The step-separation distribution approximates a Gaussian. The Gaussian, $P(x)=(1/w\sqrt{2\pi})\exp[(x-L)^2/2w^2]$, where x is the arbitrary step separation, has been shown to be an excellent approximation if the step meandering is much smaller than the average step separation L.[13] Furthermore, if the interaction energy $U(x)$ between a pair of steps can be modeled as[12,19]

$$U(x)\sim C\tau^2/x^2, \tag{1}$$

where C is a material constant and τ is either the elastic line dipole moment (torque) or the electrostatic line dipole moment along a step, the ratio of the width (standard deviation) w to the mean L of the step-separation distribution is a direct measure of the ratio of the energetic repulsion strength $A(=C\tau^2)$ to the entropic repulsion strength g via[17]

$$w/L=(g/8\pi^2A)^{1/4}. \tag{2}$$

Therefore, by comparing the measured distribution to these

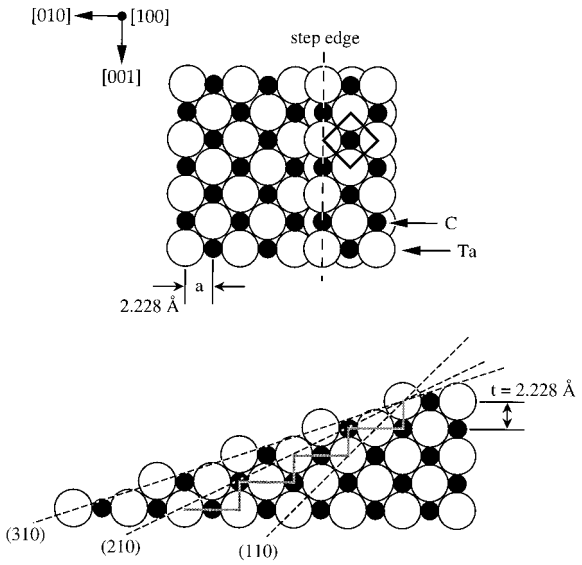

FIG. 1. A ball model of the bulk-truncated TaC(310), (210), and (110) surfaces with the lattice parameters indicated. The upper panel shows a top view from the (100) terrace normal direction, where the square unit mesh is indicated, and the lower panel shows the cross sections of these surfaces. A gray line representing the bulk-truncated (210) surface side view is also shown.

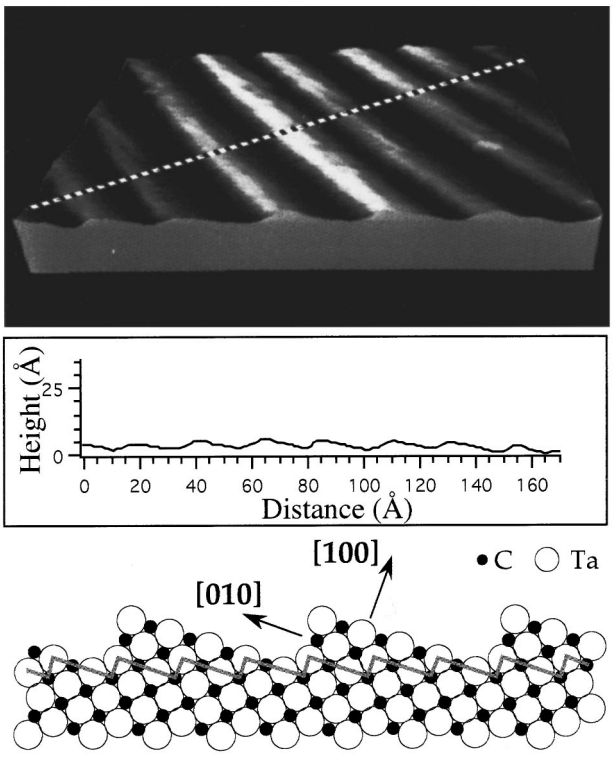

FIG. 2. The top panel is a STM image of $\sim 150 \times 105$-Å^2 area from the TaC(310) surface, where step edges are along the [001] direction. A line-cut profile from the image (indicated by the striped line) and a cross-sectional ball model for the observed surface are presented, respectively, in the middle and bottom panels. The zigzag line in the ball model represents the bulk-truncated TaC(310) surface.

theoretical predictions, one is able to gain insight into the driving force responsible for an observed surface morphology.

II. EXPERIMENT

TaC crystallizes in the sodium chloride structure and has a very high melting point, 3983 °C. The TaC(310), (210), and (110) surfaces were cut by spark erosion and polished to the desired orientations to within 0.2°. In this work, the morphologies of these surfaces were imaged by a scanning tunneling microscope at room temperature. STM measurements were conducted in an ultrahigh-vacuum chamber equipped with a conventional low-energy electron-diffraction (LEED) system. The base pressure was kept at less than 10^{-10} Torr. All STM images were taken in the constant current mode with a typical bias voltage $\sim$0.1 V and tunneling current $\sim$1 nA, using electrochemically etched Pt-Ir tips. Surface cleanliness was determined by Auger electron spectroscopy (AES) using a double-pass cylindrical mirror analyzer. The TaC surfaces were cleaned by flashing to a temperature near 2000 °C using electron bombardment, followed by slow cooling to room temperature. After cleaning, no impurities were detected with AES and a LEED pattern indicative of faceting appeared.[10] High-temperature flashing served as an activation process for the faceting. The stability of the observed structures was tested using various cooling rates from the flashing temperature. STM images show that the surfaces produced with a slower cooling rate exhibited better ordering of facets, indicating that the observed structures are the equilibrium structures. Slow cooling occurred when the heating power was gradually reduced to zero over a few minutes resulting in a cooling rate of $\sim$250 °C/min. With the heating power turned off, the sample, whose color was still red ($\sim$ 750 °C), cooled to room temperature *in situ*.

III. RESULTS

A. TaC(310)

The bulk-truncated TaC(310) surface consists of three lattice spacings ($3a$) on the (100) terrace and one lattice spacing ($t = a$) on the (010) step wall; see Fig. 1. The top panel in Fig. 2 shows a STM image from the surface. A line-cut profile obtained from it is plotted in the middle panel. From this image and dozens of others, two features can be immediately discerned: (1) Most terrace widths and step heights have been tripled from their bulk-truncated TaC(310) values, although a small number of double-height steps (and very few quadruple-height steps) are also observable in some regions. (2) The step edges are very straight, although in some areas, defects such as lateral displacements and local disordering can also be seen. A ball model representing a cross section of the observed surface is illustrated in the bottom panel of Fig. 2, where the zigzag line denotes the (310) bulk truncation. These direct STM observations are consistent with previous high-resolution LEED (HRLEED) measurements.[9]

Tripling of terrace widths and step heights can be more clearly seen from the step-separation distribution shown in Fig. 3. About 550 step separations were measured from many images of different surface areas to produce this plot. The distribution can be well fit by a Gaussian (solid curve)

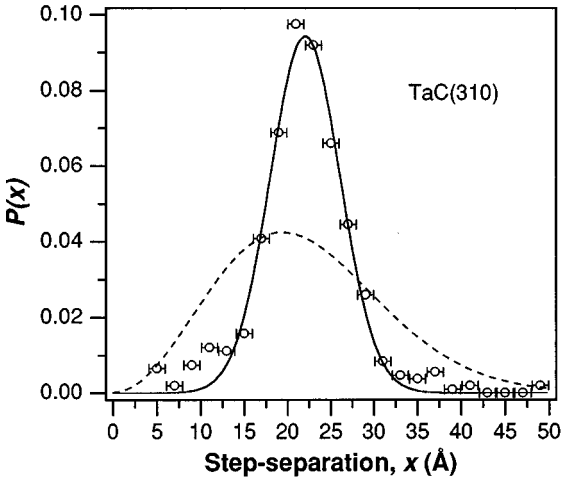

FIG. 3. Open circles denote the measured step-separation distribution for the TaC(310) surface. The solid curve is a Gaussian fit, and the dashed curve is the ''universal'' distribution (from Ref. 17) for purely entropic step repulsion.

with a mean value $L \sim 22$ Å and width $w \sim 4.03$ Å. This average step separation is in good agreement with the tripled value of the step separation for the ideal TaC(310) structure, i.e., $3\sqrt{(3a)^2+t^2}=21.14$ Å, where $a=t=2.228$ Å are the bulk-truncated surface lattice spacing and single step height (see Fig. 1), respectively. Because step edges are so straight that step edge meandering is much smaller than step separations, the Gaussian-like distribution can be used to indicate the existence of a strong step-step repulsion as described above.[13] The existence of a strong step-step repulsion can be further confirmed by comparing the universal distribution for the noninteracting TSK model;[14] see the dashed curve in Fig. 3. As can be seen, the measured distribution with $w/L=0.18$ is much narrower and sharper than the universal one with $w/L=0.42$.[14] This observation, along with the Gaussian-like distribution, enables us to unequivocally conclude that on the faceted surface, there is a strong repulsive interaction between steps.

Based on the observations above, we expect that surfaces such as TaC(210) and (110) will also exhibit similar faceting phenomenon. With this in mind, we have performed the same STM imaging and analysis on these surfaces.

B. TaC(210)

The bulk-truncated TaC(210) surface consists of two lattice spacings on the (100) terrace and one lattice spacing on the (010) step wall; see Fig. 1. From STM images, we found, surprisingly, that in some regions quadruple-height steps and eight-lattice-spacing terraces are dominant (4-8 domain), and in other regions triple-height steps and six-lattice-spacing terraces are dominant (3-6 domain). Step edges in both the 3-6 and 4-8 domains are found to be straight, as in the TaC(310) surface. Very small amounts of 5-10-type domain were also observed. Although primarily two kinds of domains coexist, the net orientation of the surface is unchanged because the ratio of average step height to average terrace width in each domain remains the same as that of the ideal surface. Shown in the top and middle panels of Fig. 4(a) are

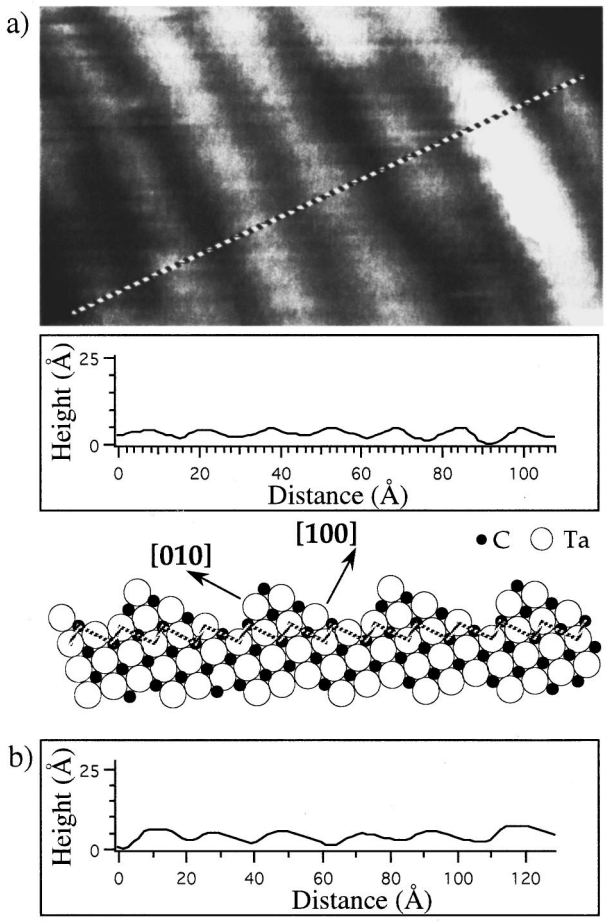

FIG. 4. (a) The top panel is a STM image of a $\sim 108\times 63$-Å^2 area from a 3-6 domain on the TaC(210) surface, where step edges are along the [001] direction. A line-cut profile from the image and a cross-sectional ball model for the observed surface are presented, respectively, in the middle and bottom panels. The zigzag line represents the bulk-truncated TaC(210) surface. (b) A line-cut profile from a 4-8 domain on the surface is shown.

a STM image obtained from a 3-6 domain and a line-cut profile from that image. A ball model representing a cross section of the observed surface is depicted in the bottom panel of Fig. 4(a). A line-cut profile from a 4-8 domain is plotted in Fig. 4(b). The size of both types of domains is in the range of 500–1000 Å, independent of annealing time at temperature ~ 800 °C as measured by HRLEED. Above that temperature, the measurement is limited by low diffraction intensities. Therefore, if a separation between these two kinds of domains were to occur, it would have to take place above this temperature.

By counting hundreds of step separations from many images in different surface areas, step-separation distributions for both domains were obtained and are plotted in Fig. 5. The surface actually contained about equal amounts of each type of step (3-6 or 4-8) as indicated by STM, and also by HRLEED measurements which will be presented elsewhere. The distributions have been well fit by two Gaussians (solid curves), one centered at $L_1 \sim 14.6$ Å and having a width $w_1 \sim 1.98$ Å, and the other centered at $L_2 \sim 19.6$ Å and having a width $w_2 \sim 4.38$ Å. Obviously, these two peaks repre-

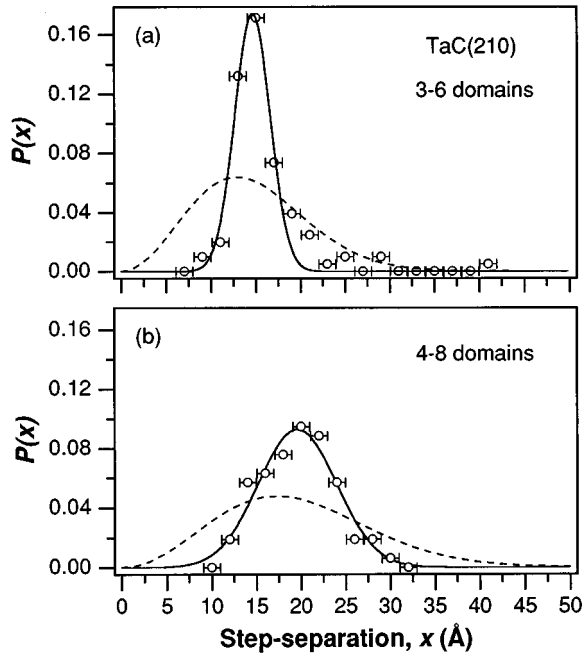

FIG. 5. Open circles denote the measured step-separation distributions for the TaC(210) surface from the two types of observed domains, (a) 3-6 and (b) 4-8. The solid curves are the Gaussian fits, and the dashed curves are the universal distributions (from Ref. 17).

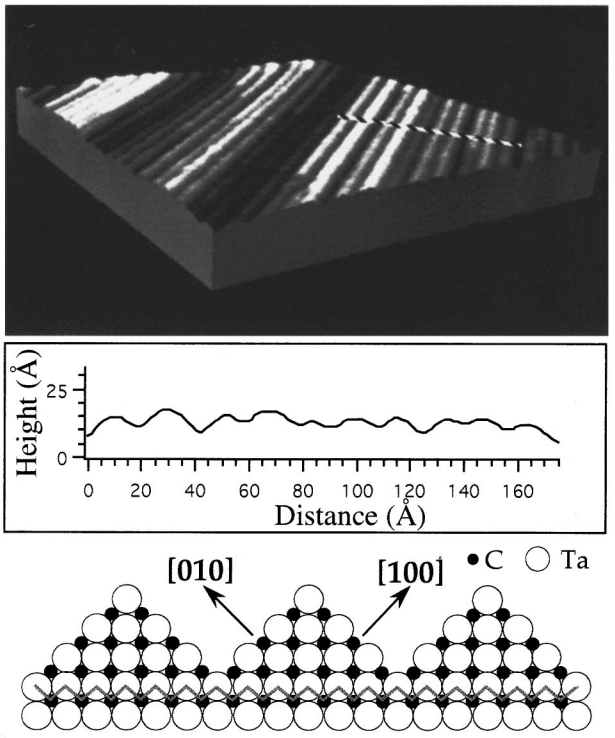

FIG. 6. The top panel is a 420×420-Å^2 STM image from the TaC(110) surface. The middle and bottom panels are a line-cut profile from the image and a ball model for the observed surface, respectively.

sent the 3-6 and 408 domains, respectively. The average step separations $L_1 \sim 14.6$ Å and $L_2 \sim 19.6$ Å are in good agreement with those of the 3-6 and 4-8 structures, i.e., $3\sqrt{(2a)^2+t^2} = 14.9$ Å and $4\sqrt{(2a)^2+t^2} = 19.9$ Å. Also, each Gaussian peak, with $w_1/L_1 \sim 0.14$ and $w_2/L_2 \sim 0.22$, is much narrower than the universal distribution ($w/L = 0.42$); see the dashed curves in Fig. 5. These two narrow Gaussian peaks indicate the existence of a strong step-step repulsion in both the 3-6 and 4-8 domains. This situation is similar to that of the TaC(310) surface, except for the coexistence of the two dominant step separations, which could be due to a near-energy degeneracy of the 3-6 and 4-8 structures.

C. TaC(110)

The TaC(110) surface can be viewed as one lattice spacing on the (100) terrace and one lattice spacing on the (010) step wall; see Fig. 1. From STM images, we found that the TaC(110) surface is likewise faceted into a hill-and-valley array, with straight step edges running along the [001] direction. Defects similar to those observed on the other two surfaces also exist. The middle panel of Fig. 6 shows a line-cut profile from the top-panel STM image. A ball model representing a cross section of the observed surface is depicted in the bottom panel. As can be seen, the rippling array is not completely regular, but each hill appears to be symmetric, with a complete absence of (110) terraces. By counting about 500 step separations from many large-area images in different surface regions, a step-separation distribution was obtained and is shown in Fig. 7. As before,the distribution can be well fit by a Gaussian (solid curve) with the mean value $L \sim 18.7$ Å and width $w \sim 3.26$ Å. The mean value $L \sim 18.7$ Å is in good agreement with that of the 6-6 structure, i.e., $6\sqrt{a^2+t^2} = 18.9$ Å, and is consistent with our previous HR-LEED measurements.[10] Once again, the Gaussian-like distribution ($w/L \sim 0.17$) is much narrower than the universal distribution ($w/L \sim 0.42$, dashed curve), indicating the existence of a strong step-step repulsion.

IV. DISCUSSION

The structures we observed on these TaC surfaces are the equilibrium phases slowly quenched through the diffusion cutoff temperature (probably near 800 °C). From the analyses above, we have concluded that, after faceting has occurred, there exists a strong step-step repulsion on these surfaces. In fact, by using Eq. (2) and the measured ratios of w/L, the ratio A/g has been calculated, suggesting that on the faceted surfaces, the step-step energetic repulsion is between 5.4 and 33 times as large as the entropic step repulsion depending on the surface orientation. It is natural to assume that the integrated repulsion energy on these surfaces would be much larger for the high-step-density bulk-truncated surfaces, and that this reduction in energy drives the faceting on these surfaces. This can be explained as follows: Eq. (1) indicates that the interaction between a pair of steps is due to either the electrostatic line dipoles or elastic line dipoles

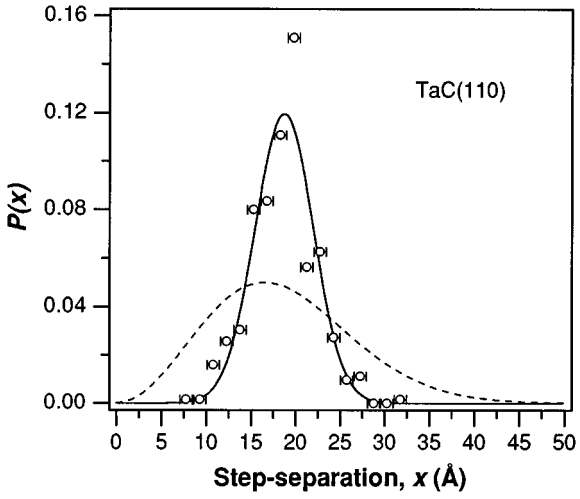

FIG. 7. Open circles are the measured step-separation distribution on the TaC(110) surface. The solid curve is a Gaussian fit, and the dashed curve is the universal distribution (from Ref. 17).

(torques) at steps with zero moments on terraces.[12,19] The electrostatic dipoles at steps on a clean surface are usually caused by electronic charge-density distortions, as have been observed on certain elemental metal surfaces.[20,21] On the surfaces of ionic crystals like TaC, the charge density is more localized, and therefore the electrostatic effect might not be as significant as the elastic effect. However, previous LEED (Ref. 22) and x-ray photoelectron spectroscopy (XPS) (Ref. 23) studies independently suggest that on the TaC(100) surface there is a charge redistribution between carbon and tantalum atoms. If this charge redistribution produces a nonzero electrostatic dipole at steps on the TaC(310), (210), and (110) surfaces, the dipole component normal to the (100) terrace, $\tau_s = qh$, where q is the charge associated with the dipole and h is the total step height, will induce a repulsive step-step interaction.[12] The elastic dipoles at steps are created by strain fields, i.e., $\tau_e = \sigma h$,[19] where σ is the surface tension. We then propose that, regardless of whether the dipoles at steps are electrostatic or elastic, they will be proportional to the total step height h. Assuming q and σ are unchanged from before to after faceting,[17] as step separation increases m times , the step height increases m times as does the dipole moment. Then, according to Eq. (1), faceting would have no effect on the repulsive energy between a pair of steps. Although there is no reduction in a given step pair's repulsive energy, the observed surface reorderings show an m-fold reduction in the total number of step pairs, and hence the total step repulsive energy on the surface reduces by $1/m$ after the faceting.

One question immediately raised is why the phase separation does not continue to form an even larger terrace width and step height to further reduce the surface's total step repulsive energy. We suggest that the increase in total step formation energy due to further increasing the step height would exceed the decrease in total step repulsive energy due to decreasing the number of step pairs. A balance between these two factors determines the average step separation. As mentioned earlier, we speculate that on the (210) surface, the minimization of this energy balance has two degenerate solutions, resulting in the coexistence of two different domain types, 3-6 and 4-8. However, quantitative information for the final selection of facet sizes requires a detailed total-energy minimization calculation which is beyond our experimental scope. We hope that our experimental work will stimulate a theoretical interest in ionic crystal surfaces.

The faceting observed above involves large mass transport. This process can only be activated by heating the surfaces above some temperature. We believe that this has occurred during sample cleaning. Cleaning requires the sample to reach ~2000 °C, which should already be above the activation temperature for the faceting. It can be imagined that as the clean surface is cooled from high temperature, single-height steps coalesce to form facets. This coalescence has been observed in a similar faceting process on the TaC(910) surface, and will be published elsewhere. Meanwhile, as facets grow laterally along the step-edge direction, step-edge meandering is suppressed by the strong nearest-neighbor bonds of step atoms and by the strong step-step repulsion. In this case, the former could play the major role because TaC has a very high melting point, and its ionic bonds are expected to be very strong. Lateral displacements of step edges observed in some STM images could thus be due to the misaligned intersection of two adjacent growing facets.

V. SUMMARY

We have studied the structural stability of the TaC(310), (210), and (110) surfaces with STM, and find that the bulk-truncated surfaces are unstable and facet into hill-and-valley structures comprised of enlarged (100) terraces and (010) step walls after high-temperature flashing. By measuring the equilibrium step-separation distributions on these surfaces, we determined that a strong energetic repulsion exists between steps which dominates the entropic step repulsion. This is inferred by comparing the measured Gaussian-like distributions to a universal distribution for the noninteracting TSK model. We suggest that the faceting is driven by a lowering of the total step repulsive energy through a reduction of the total number of step pairs. Future experiments (in progress) involving the study of single-height step interactions on slightly misoriented (100) surfaces will give more insight into the driving force of the faceting. Also, more experiments are still required to distinguish whether the repulsive interaction between steps owes to the electrostatic or elastic effect, and to study the kinetics of facet formation.

ACKNOWLEDGMENTS

We thank T. L. Einstein for invaluable comments on our manuscript and discussions and for providing the theoretical curve of the ''universal'' distribution, Woei Wu (Larry) Pai for his helpful suggestions, and R. J. Warmack for his help during the initial STM setup. This research was sponsored by the Division of Materials Sciences, U.S. Department of Energy under Contract No. DE-AC05-84OR21400 with Lockheed-Martin Energy Systems, Inc.

[1] G. Wulff, Kristallografiya **34**, 449 (1901).
[2] C. Herring, Phys. Rev. B **2**, 87 (1951).
[3] R. Koch, M. Borbonus, O. Haase, and K. H. Rieder, Phys. Rev. Lett. **67**, 3416 (1991).
[4] J. Falta, R. Imbihl, and M. Henzler, Phys. Rev. Lett. **64**, 1409 (1990).
[5] J. S. Ocomert, W. W. Pai, N. C. Bartelt, and J. E. Reutt-Robey, Phys. Rev. Lett. **72**, 258 (1994).
[6] H. Hibino and T. Ogino, Phys. Rev. Lett. **72**, 657 (1994).
[7] E. Hahn, H. Schief, V. Marsico, A. Fricke, and K. Kern, Phys. Rev. Lett. **72**, 3378 (1994).
[8] G. M. Watson, Doon Gibbs, D. M. Zehner, Mirang Yoon, and S. G. Mochrie, Phys. Rev. Lett. **71**, 3166 (1993).
[9] J.-K. Zuo and D. M. Zehner, Phys. Rev. B **46**, 16 122 (1992).
[10] J.-K. Zuo, R. J. Warmack, D. M. Zehner, and J. F. Wendelken, Phys. Rev. B **47**, 10 743 (1993); J.-K Zuo, D. M. Zehner, J. F. Wendelken, R. J. Warmack, and H.-N. Yang, Surf. Sci. **301**, 233 (1994).
[11] C. Rottman and M. Wortis, Phys. Rep. **103**, 59 (1984).
[12] C. Jayaprakash, C. Rottman, and W. F. Saam, Phys. Rev. B **30**, 6549 (1984).
[13] N. C. Bartelt, T. L. Einstein, and E. D. Williams, Surf. Sci. **240**, L591 (1990).
[14] B. Joós, T. L. Einstein, and N. C. Bartelt, Phys. Rev. B **43**, 8153 (1991).
[15] E. Pehlke and J. Tersoff, Phys. Rev. Lett. **67**, 465 (1991).
[16] A. C. Redfield and A. Zangwill, Phys. Rev. B **46**, 4289 (1992).
[17] E. D. Williams, R. J. Phaneuf, Jian Wei, N. C. Bartelt, and T. L. Einstein, Surf. Sci. **294**, 219 (1993); **310**, 451 (1994).
[18] M. E. Fisher and D. S. Fisher, Phys. Rev. B **25**, 3192 (1982).
[19] V. I. Marchenko and A. Y. Parshin, Zh. Eksp. Teor. Fiz. **79**, 257 (1980) [Sov. Phys. JETP **52**, 129 (1980)].
[20] B. Krahl-Urban, E. A. Niekisch, and H. Wagner, Surf. Sci. **64**, 52 (1977).
[21] M. D. Thompson and M. B. Huntington, Surf. Sci. **116**, 522 (1982).
[22] J. R. Noonan, H. L. Davis, and G. R. Gruzalski, J. Vac. Sci. Technol. A **5**, 787 (1987).
[23] G. R. Gruzalski, D. M. Zehner, J. R. Noonan, H. L. Davis, R. A. DiDio, and K. Müller, J. Vac. Sci. Technol. A**7**, 2054 (1989).